PRAMANA — journal of physics

Vol. 69, No. 5
November 2007
pp. 895–901

Event-shape of dileptons plus missing energy at a linear collider as a supersymmetry/Arkani-Hamed–Dimopoulos–Dvali discriminant

PROBIR ROY
Tata Institute of Fundamental Research, Homi Bhabha Road, Mumbai 400 005, India
E-mail: probir@theory.tifr.res.in

Abstract. An event-shape analysis of the dileptons in the process $e^+e^- \rightarrow \ell^+\ell^-\not{E}$, studied in ILC or CLIC, can clearly discriminate between a supersymmetric or a large extra dimensional (ADD) production mechanism.

Keywords. Linear collider; supersymmetry; large extra dimensions; event-shape.

PACS Nos 04.50.+h; 11.10.Kk; 11.25.Mj; 12.60.Jv; 13.66.Hk; 14.80.Ly

1. Objective

This talk is based on work done with Partha Konar [1]. New physics is widely expected to emerge at TeV energies on the basis of naturalness, gauge hierarchy and WIMP dark matter considerations. Among possible scenarios, supersymmetry (SUSY) [2] and large extra dimensions [3] of the Arkani-Hamed–Dimopoulos–Dvali (ADD) model [4] are in the limelight. This is because they promise a large number of new states to be explored at the LHC as well as ILC and CLIC. The signature of these states is the occurrence of multilepton, multijet events with a large missing energy $\not{E}$ or missing transverse energy $\not{E}_{\rm T}$. The question of discrimination between the two scenarios on the basis of such events is thus an important issue.

2. Signal cross-section

We consider the lepton sector where the LHC will not be a powerful probe. Hence we zero in on ILC ($\sqrt{s}$ = 500 GeV) and CLIC ($\sqrt{s}$ = 3 TeV). Our process is $e^+e^- \rightarrow \ell^+\ell^-\not{E}$, where ℓ is an electron or a muon. For SUSY, we take the MSSM with the parameters $\tan\beta$, $m_{\tilde{e}_{\rm L,R}}$, $m_{\tilde{\mu}_{\rm L,R}}$, μ, M_1 and M_2 in standard notation, with all mass parameters expected to be $\gtrsim \mathcal{O}$ (100 GeV). The production of a pair of charged sleptons $\tilde{\ell}^{\pm}_{\rm L,R}$ and their subsequent decays into $\ell^{\pm}\tilde{\chi}^0_1$ lead to our signal in this scenario. Signal sensitivity to $\tan\beta$ turns out to be very mild and we fix the

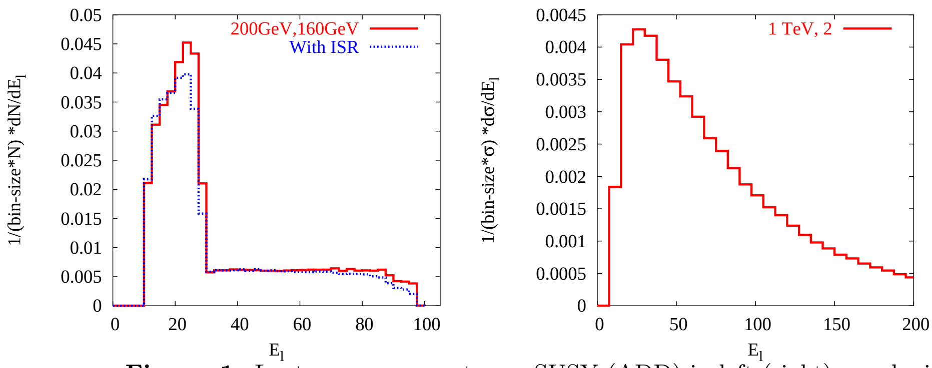

Figure 1. Lepton energy spectrum: SUSY (ADD) in left (right) panel with M_2 and M_1 ($M_{\rm S}$ and d) specified.

latter at 10. Thus we have a 4-parameter SUSY model. Turning to the ADD case, we take d extra spatial dimensions (with $d = 2, 3, 4, 5$), all compactified on a d-torus with the same radius $R_{\rm c}$ of compactification for each. All standard model fields are assumed to lie on a 3-brane while only gravity is taken to propagate in the bulk. The parameters $d, R_{\rm c}$ and the fundamental 'string' scale $M_{\rm S}$ in higher dimensions are related by $M_{\rm S}^{2+d} = (4\pi)^{d/2}\Gamma(d/2)G_{\rm N}^{-1}R_{\rm c}^{-d}$, $G_{\rm N}$ being Newton's constant, so that one can take d and $M_{\rm S}$ to be the two independent parameters of this model.

A reliable discriminant between the SUSY and ADD scenarios, apart from being a measurable quantity, needs to have robust features distinguishing between them. Such is not the case with the lepton energy spectrum here. For appropriate parameters and with ISR corrections, the famous box-shaped lepton energy spectrum from slepton decay can get squeezed [5] into a hump (figure 1a), not too unlike that in the ADD case (figure 1b). Lepton angular distributions also tend to be flat and somewhat similar in both scenarios for most of the allowed range. In contrast, event-shape distributions like those of sphericity and thrust are robust with respect to ISR/FSR corrections and differ significantly for the two scenarios.

All lowest-order diagrams, relevant to the process $e^+e^- \to \ell^+\ell^- \not{E}$ in the ADD (SUSY) case are shown in the left (right) panel of figure 2. For the former, one can write

$$\sigma(e^+e^- \to \ell^+\ell^- \not{E}) = \Sigma_n \sigma(e+e^- \to \ell^+\ell^- G_n)$$
$$\simeq \int_0^{\sqrt{s}} {\rm d}m\ \sigma(m)\left[2R_{\rm c}^d m^{d-1}(4\pi)^{-d/2}/\Gamma(d/2)\right],$$

m being the mass of the graviton mode with $\sigma(m)$ being the corresponding production cross-section. The latter has been calculated with the subroutine HELAS. For the SUSY case, the rate for the process $e^+e^- \to \tilde{\ell}^+_{\rm L,R}\tilde{\ell}^-_{\rm L,R} \to \ell^+\ell^-\tilde{\chi}^0_1\tilde{\chi}^0_1$ has been calculated using the package COMPHEP. Typical cross-sections for the two scenarios, computed with cuts described in the next section, are listed in table 1. Values for SUSY and ADD show considerable overlap both for ILC (upper half) and CLIC (lower half).

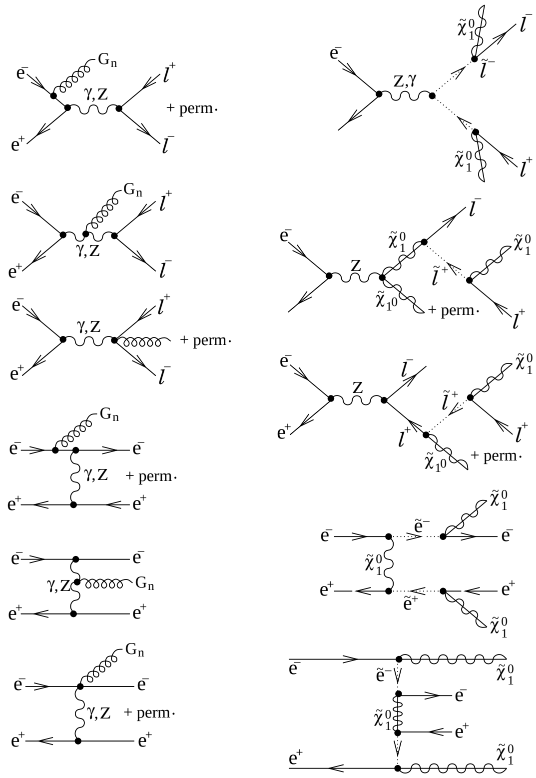

Figure 2. Lowest-order diagrams for our process in the two cases.

3. SM background and chosen cuts

The main background to our signal comes from the reactions $e^+e^- \to \ell^+\ell^- Z$, $Z \to \nu_\ell \bar{\nu}_\ell$ and $e^+e^- \to W^+W^-$, $W \to \ell\nu_\ell$. The first can be eliminated by a missing mass cut clearly excluding M_Z. The second is kinematically reconstructible, modulo a 2-fold ambiguity, and can then be explicitly subtracted. The signal-to-background ratio gets further enhanced on account of our cuts chosen as follows. (1) Each ℓ must be at least 10° from the beam pipe to control beamsstrahlung effects and collinear singularities from t-channel photon exchange. (2) For each ℓ, p_{T}^{ℓ} must exceed 10 GeV (ILC) or 20 GeV (CLIC). (3) The corresponding acceptance lower limits for $p_{\mathrm{T}}^{\mathrm{miss}}$ are chosen as 15 GeV and 25 GeV respectively. (4) The isolation criterion $\Delta R \equiv (\Delta\eta^2 + \Delta\phi^2)^{1/2} > 0.2$ is chosen. (5) The opening angle acceptance range is taken as $5° < \theta_{\ell^+\ell^-} < 175°$. (6) The missing mass cut is chosen to be $M_{\mathrm{miss}} > 150$ GeV for ILC and 450 GeV for CLIC. With these cuts, the SM background is about 36 fb (ILC) and 72 fb (CLIC) to be compared with the signal numbers in table 1. For an integrated luminosity of 100 fb^{-1} (ILC) and 1000 fb^{-1} (CLIC), a minimum signal cross-section of 1.8 fb and 0.8 fb would achieve $S/\sqrt{B} \simeq 3$.

Table 1. Cross-sections for various parameters of the two scenarios.

σ_{SUSY} (fb)						σ_{ADD} (fb)				
$\tan\beta = 10$		m_{slep} (GeV)				M_{S} (TeV)				
M_2, M_1 (GeV)	μ (GeV)	155	205	225	245	0.75	1.0	1.5	2.0	d
200, 100	−400	427	164	59	7.8	1090	345	68	22	2
300, 150	−400	144	137	75	19	455	108	14	3.3	3
400, 200	−150	92	40	13	0.6	202	36	3.2	0.6	4
400, 200	−100	79	32	6.9	0.3	97	13	0.8	0.1	5
σ_{SUSY} (fb)						σ_{ADD} (fb)				
$\tan\beta = 10$		m_{slep} (GeV)				M_{S} (TeV)				
M_2, M_1 (GeV)	μ (GeV)	700	800	900	1000	4.5	5.0	5.5	6.0	d
200, 100	−500	24	19	15	11	124	81	56	39	2
400, 190	−500	22	18	15	11	58	34	21	14	3
600, 290	−500	21	16	13	10	31	16	9.2	5.5	4
800, 380	−500	21	18	12	8	17	8.3	4.2	2.3	5

SM bkgd $\sim$ 36 fb (72 fb).

4. Event-shape variables

The idea of using event-shape variables arises from the following expectation. Decay products from a slepton pair, produced not far from threshold, are likely to be more isotropic as compared with the somewhat more spiked configurations of bremsstrahlung-like graviton emission in the ADD case. We define a sphericity tensor S_{ij} and a scalar parameter thrust T as

$$S_{ij} = \frac{p^i_{\ell^+} p^j_{\ell^+} + p^i_{\ell^-} p^j_{\ell^-}}{\mathbf{p}^2_{\ell^+} + \mathbf{p}^2_{\ell^-}}, \quad T = \max \frac{\hat{\mathbf{n}} \cdot (\mathbf{p}_{\ell^+} + \mathbf{p}_{\ell^-})}{|\mathbf{p}_{\ell^+}| + |\mathbf{p}_{\ell^-}|},$$

where the thrust axis unit vector $\hat{\mathbf{n}}$ is chosen to maximize the numerator of T. The allowed range for the latter is $1/2 \leq T \leq 1$ and a spiked (isotropic) event has $T \sim 1$ (1/2). On the other hand, if $\lambda_{1,2,3}$ are the eigenvalues of S_{ij}, defined with $\lambda_1 \geq \lambda_2 \geq \lambda_3 \geq 0$, $\lambda_1 + \lambda_2 + \lambda_3 = 1$, the sphericity S of the event can be defined as

$$S = \frac{3}{2}(\lambda_2 + \lambda_3)$$

with $0 \leq S \leq 1$, where $S = 1, 0$ for an ideally spherical, linear event. For our process, the planar nature of two-body production implies that $\lambda_3 = 0$. Thus the shape of an isotropic event is circular (rather than spherical) for $S_{\max} = 3/4$. However, ISR/FSR effects can, in principle, push S beyond the maximum and towards unity.

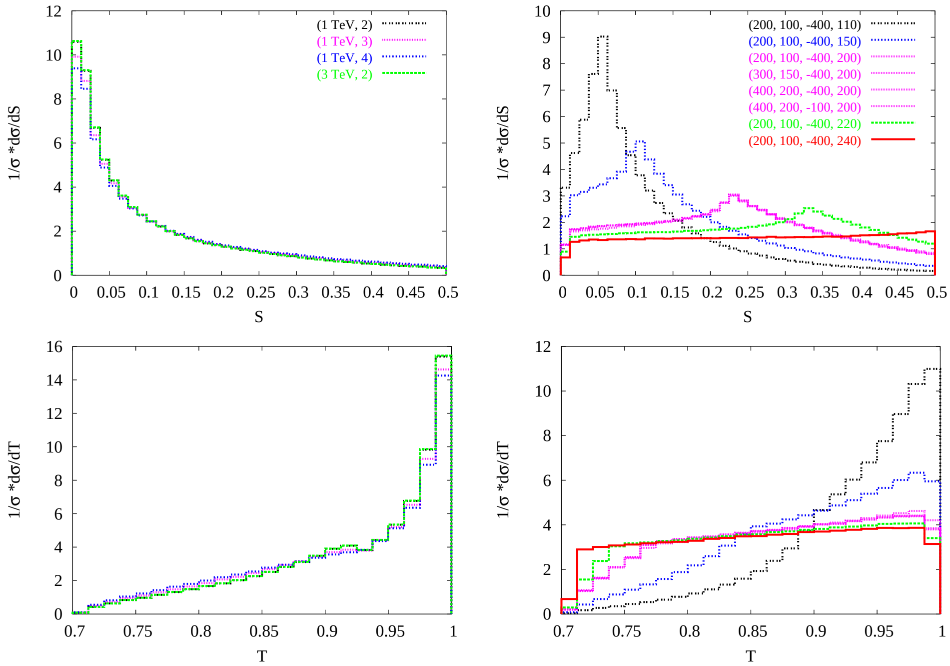

Figure 3. Sphericity (upper panels) and thrust (lower panels) distributions for ADD (left) and SUSY (right) at ILC.

5. Results and discussion

The resultant sphericity and thrust distributions for the two scenarios relevant to ILC is shown in figure 3 and CLIC is shown in figure 4. We have cross-checked the SUSY plots by redoing [1] the calculation in PYTHIA with ISR/FSR effects taken into account. The observed changes are small, showing the robustnes of these event-shape variables with respect to such corrections.

An examination of these plots clarifies the distinction between the two scenarios. Both S and T distributions are flatter in the SUSY case, showing structure in terms of a peak in S and a break in T. In contrast, they are monotonic for ADD with maxima at $S = 0$ and $T = 1$ (spiked event), followed by a continuous fall and rise respectively. It is a fact that the discrimination is more spectacular via S than via T. In the SUSY case, the location of the sphericity peak is uniquely correlated with the slepton mass $m_{\tilde{\ell}}$, being insensitive to other MSSM parameters. This is demonstrated in the scatter plot of figure 5 displaying the cross-section against the said location. In contrast, the maxima for all ADD parametric choices are strictly at $S = 0$.

In summary, a clear discrimination between SUSY and ADD will be possible in $e^+e^- \to \ell^+\ell^- \not{E}$ at a linear collider by means of ISR/FSR-insensitive sphericity distributions. A peaked structure, with the peak location uniquely specifying the slepton mass, characterizes SUSY. In contrast, a structureless monotonic fall-off from a maximum at $S = 0$ is the hallmark of ADD.

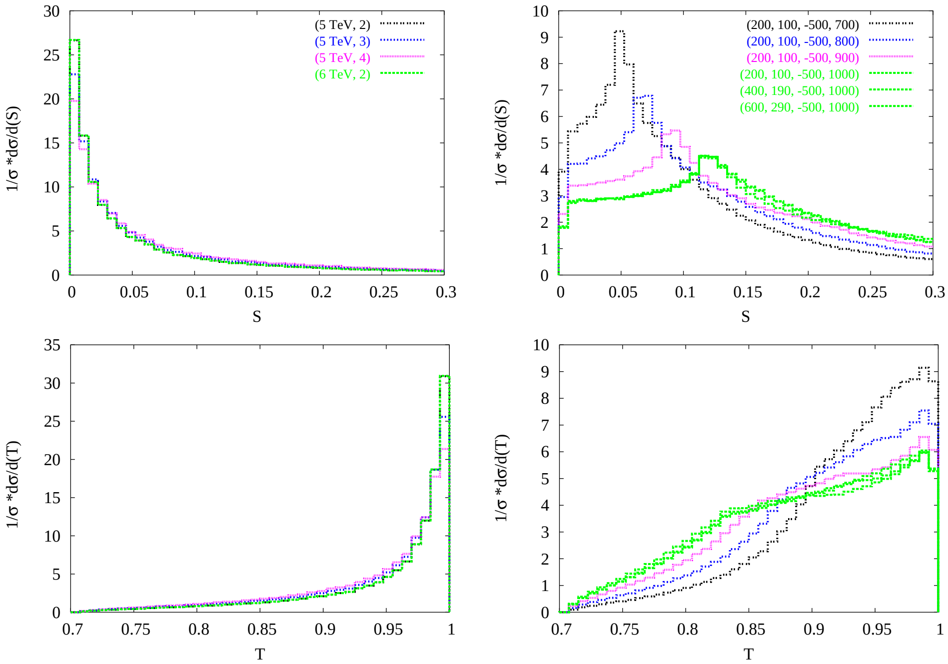

Figure 4. Sphericity (upper panels) and thrust (lower panels) distributions for ADD (left) and SUSY (right) at CLIC.

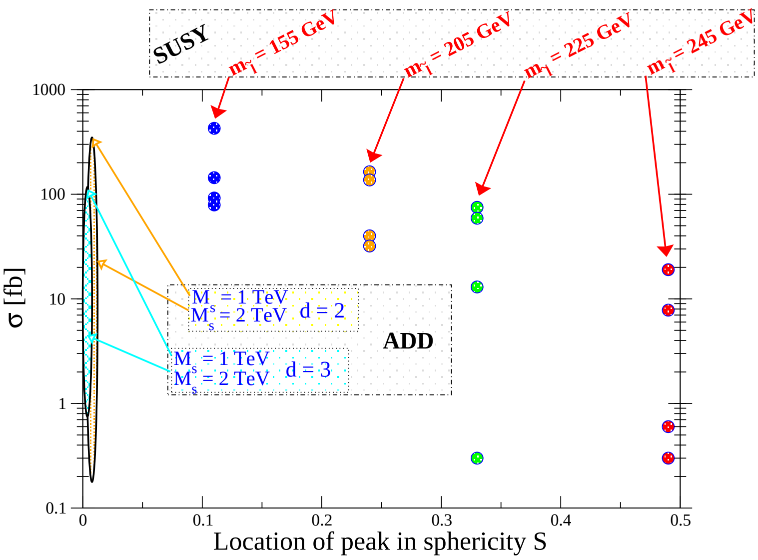

Figure 5. Sphericity peak location.

References

[1] P Konar and P Roy, *Phys. Lett.* **B634**, 295 (2006)
[2] M Drees, R M Godbole and P Roy, *Theory and phenomenology of sparticles* (World Scientific, Singapore, 2004)
[3] A Perez-Lorenzana, *J. Phys. Conf. Ser.* **18**, 224 (2005)
[4] I Antoniadis, *Phys. Lett.* **B246**, 377 (1990)
N Arkani-Hamed *et al*, *Phys. Lett.* **B429**, 263 (1998); *Phys. Rev.* **D59**, 086004 (1999)
[5] M Battaglia *et al*, *J. High Energy Phys.* **0507**, 033 (2005)